

Supporting Information

High-efficiency organic light-emitting diodes based on cationic iridium(III) complexes with double tridentate ligands

Yang Kang,^{†a} Sheng Ren,^{†b} Zhao Zhi Ying,^{†a} Tong Bi-Hai,^{*a,c} Chen Ping^{*b} and Kong Hui^{*a}

^a School of Metallurgy Engineering, Anhui University of Technology, Maanshan, 243002, Anhui, China. E-mail: tongbihai@163.com, konghui@ahut.edu.cn.

^b Shandong College Laboratory of Optoelectronic Functional Materials and Optoelectronic Devices, Institute of Science and Technology for Opto-Electronic Information, Yantai University, Yantai, 264005, Shandong, China. E-mail: pingchen@jlu.edu.cn.

^c State Key Laboratory of Coordination Chemistry, Nanjing University, Nanjing, 210023, China.

[†] These authors contributed equally to this work.

* Corresponding authors.

Contents:

1. General descriptions
2. The supplementary crystallographic data
3. Photophysical properties
4. The supplementary device data
5. The ¹H/¹⁹F-NMR and high-resolution mass spectrometers (HRMS) spectra of all new compounds
6. References

1. General descriptions

1.1. Materials and characterization

All the materials and solvents were obtained commercially and used as received without further purification. Proton NMR spectra were measured on a Bruker AV400 spectrometer. High resolution mass spectra (HRMS) were recorded with a TOF 5600^{plus} mass spectrometer. X-ray crystallography diffraction was carried out on a Bruker SMART Apex CCD diffractometer. Cyclic voltammetry (CV) was measured on a CHI1140B Electrochemical Analyzer through a three-electrode system with a glassy carbon disk as the working electrode, platinum plate as the counter electrode and Ag/AgCl as the reference electrode. UV/Vis absorption spectra were recorded on a Purkinje General TU-1901 spectrophotometer. The PL spectra were recorded on a PerkinElmer LS-55 fluorescence spectrophotometer. The PL quantum efficiency and lifetime were measured with an Edinburgh FLS980 instrument.

1.2. Computational methodology

B3LYP functional was used to optimize the geometrical structures of ground state (S_0).^[1] A “double- ξ ” quality basis set consisting of Hay and Wadt’s effective core potentials (ECP), LANL2DZ,^[2] was employed to the Ir atom. 6-31G(d) basis set^[3] was applied to other nonmetallic atoms. The solvent effect in CH_2Cl_2 medium was considered throughout the calculations. Combined with VMD program,^[5] the molecular orbital was visualized by Multiwfn code.^[4] The frontier molecular orbital (FMO) distribution in molecules was analyzed by Multiwfn using Mulliken population analysis. Gaussian 16 software package was used for calculations.^[6]

1.3. OLED fabrication

In a general procedure, indium tin oxide (ITO)-coated glass substrates were etched, patterned, and washed with detergent, deionized water, acetone, and ethanol in turn. For vacuum-deposited OLEDs, the ITO substrate was loaded in a deposition chamber and conducted with the treatment of ultraviolet ozone. Vacuum chambers were employed to deposit metal layer and organic layer, and the base pressure was higher than 8×10^{-5} Pa. For spin-coating OLEDs, PEDOT:PSS was spin-coated to smooth the ITO surface and to promote hole injection, and then the emissive layer was spin-coated from a chlorobenzene solution, on which an electron-transporting/hole-blocking layer

and metal layer were deposited in a vacuum chamber at a pressure of 8×10^{-5} Pa. EL spectra were collected on a Spectra Scan PR655 photometer. Current density–voltage–luminance (J-V-L) measurements were recorded simultaneously using a Keithley 4200 semiconductor parameter analyzer coupled with a Newport Multi-Function 2835-C optical meter, which measured luminance in the forward direction. All device characterizations were carried out under ambient laboratory conditions at room temperature without encapsulation.

2. The supplementary crystallographic data.

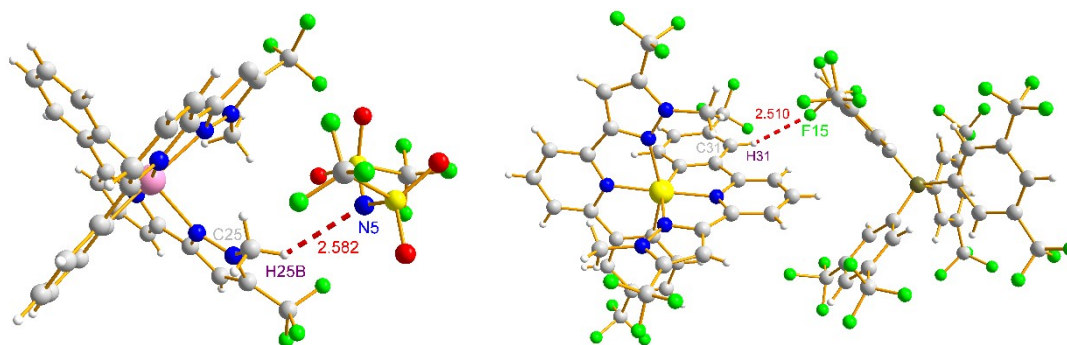


Fig. S1 Intramolecular hydrogen bonds in the single crystal of complexes **1b** (left, H(25B)-N(5) = 2.582 Å, \angle C(25)-H(25B) \cdots N(5) = 138 °) and **2** (right, H(31)-F(15) = 2.510 Å, \angle C(31)-H(35) \cdots F(15) = 158 °).

Table S1 Crystallographic and refinement data for complexes

	1b	2
Empirical formula	C ₃₄ H ₂₂ F ₁₂ IrN ₇ O ₄ S ₂	C ₆₆ H ₃₂ BF ₃₆ IrN ₆
Formula weight	1076.90	1795.98
Temperature/K	296.15	296(2)
Crystal system	orthorhombic	monoclinic
Space group	P212121	P2 ₁ /c
a/Å	9.4185(11)	13.152(3)
b/Å	11.7390(14)	18.686(5)
c/Å	34.800(4)	28.086(7)
α /°	90	90
β /°	90	90.010(10)
γ /°	90	90
Volume/Å ³	3847.6(8)	6902(3)
Z	4	4
ρ calcg/cm ³	1.859	1.728
μ /mm ⁻¹	3.686	2.078

F(000)	2096.0	3504.0
Crystal size/mm ³	0.23 × 0.21 × 0.2	0.22 × 0.2 × 0.18
Radiation	MoK α (λ = 0.71073)	MoK α (λ = 0.71073)
2 θ range for datacollection/ $^{\circ}$	4.48 to 54.946	4.056 to 52.096
Index ranges	-12 \leq h \leq 12, -13 \leq k \leq 15, -39 \leq l \leq 45	-16 \leq h \leq 16, -20 \leq k \leq 22, -34 \leq l \leq 30
Reflections collected	24328	38472
Independent reflections	8669 [R _{int} = 0.0311, R _{sigma} = 0.0559]	13448 [R _{int} = 0.0457, R _{sigma} = 0.0541]
Data/restraints/parameters	8669/562/544	13448/1081/993
Goodness-of-fit on F ²	1.066	1.029
Final R indexes [$I \geq 2\sigma(I)$]	R ₁ = 0.0320, wR ₂ = 0.0596	R ₁ = 0.0554, wR ₂ = 0.1464
Final R indexes [all data]	R ₁ = 0.0386, wR ₂ = 0.0614	R ₁ = 0.0852, wR ₂ = 0.1631
Largest diff. peak/hole / e \AA^{-3}	0.63/-1.72	1.62/-0.96

3. Photophysical properties

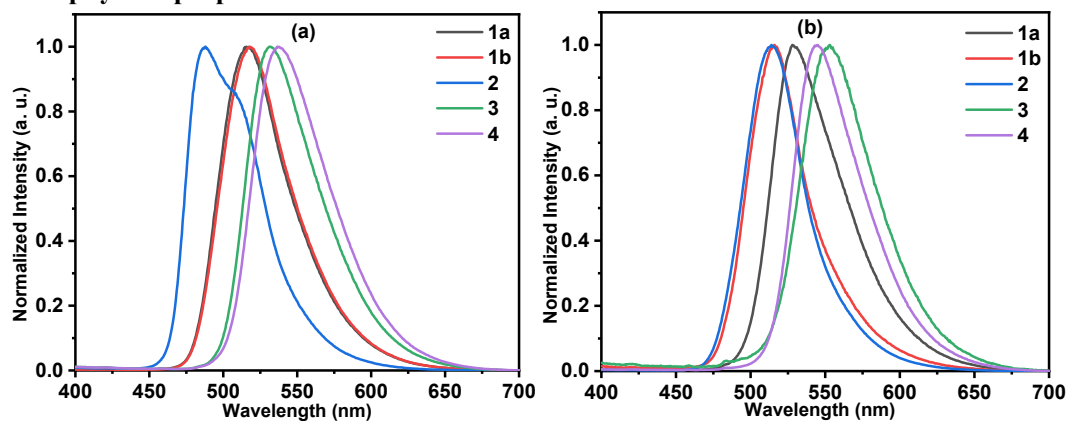


Fig. S2 The PL spectra of as-prepared complexes in PMMA films (1 wt%), (a) and in neat powder (b).

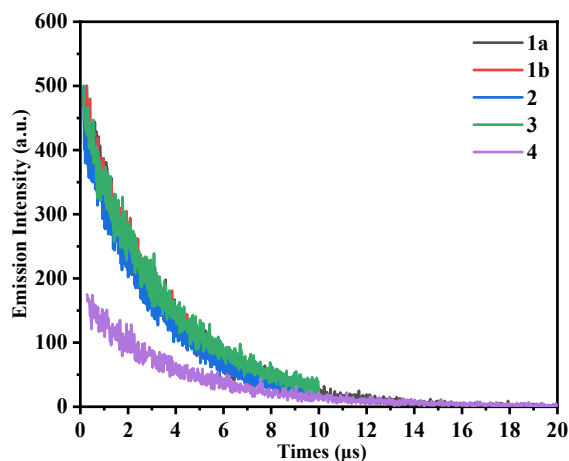


Fig. S3 The emission decay curves of as-prepared complexes in PMMA films at a conc. of 1 wt%.

4. The supplementary device data

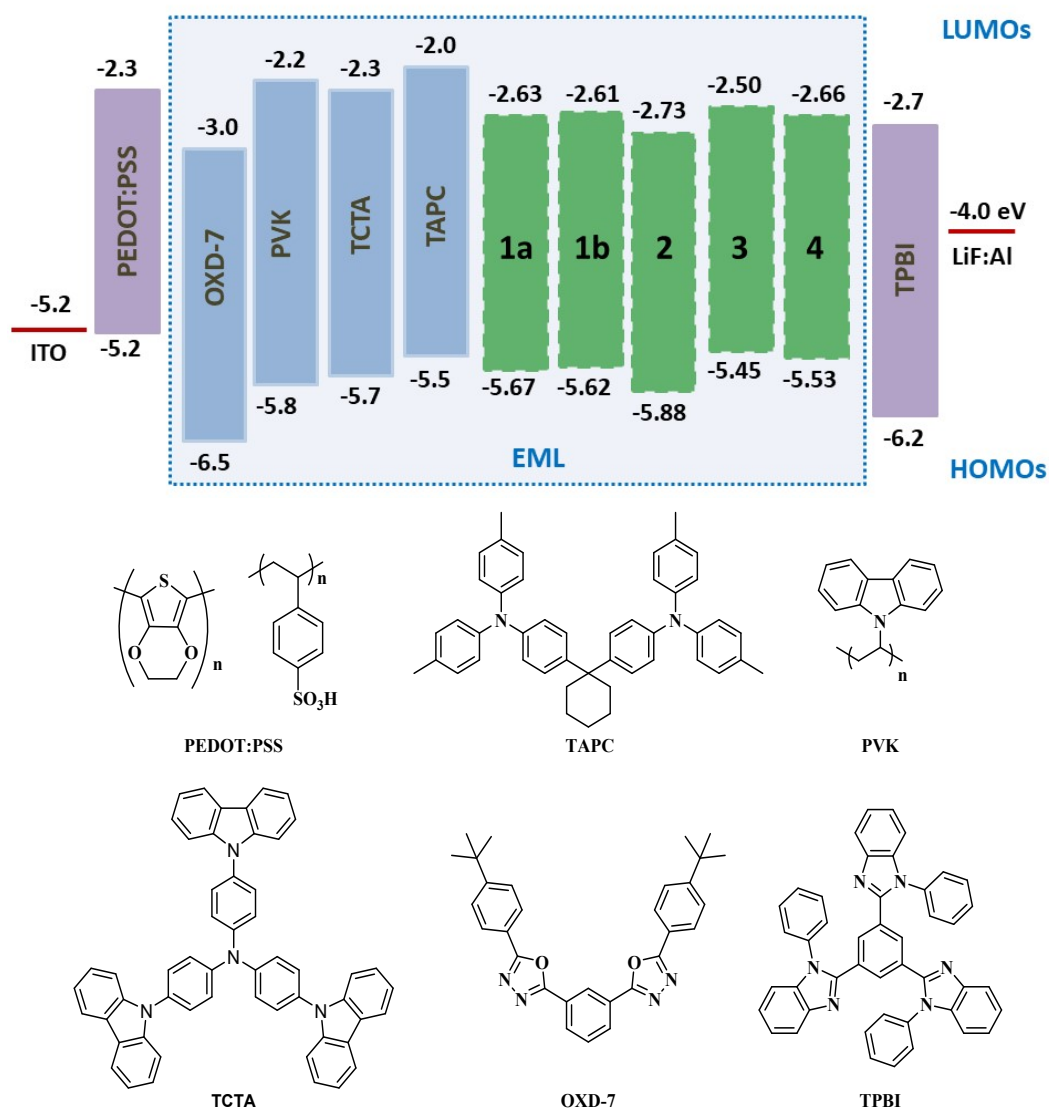


Fig. S4 Energy level diagram and the molecular formula of materials used in OLED devices.

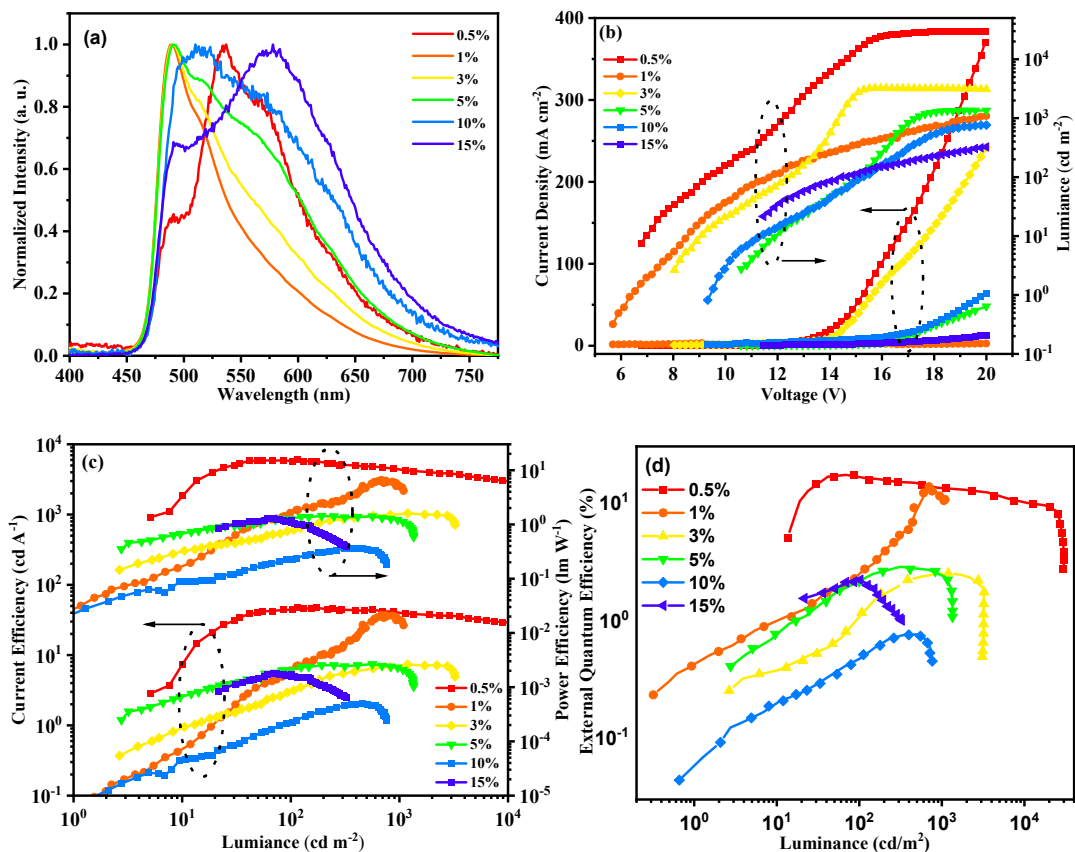


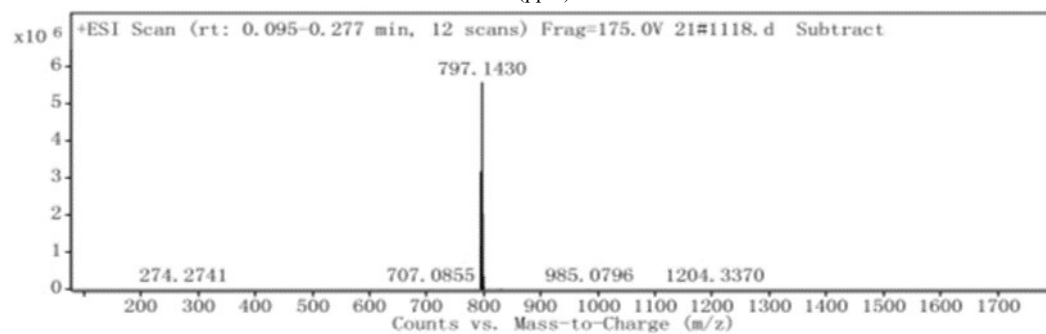
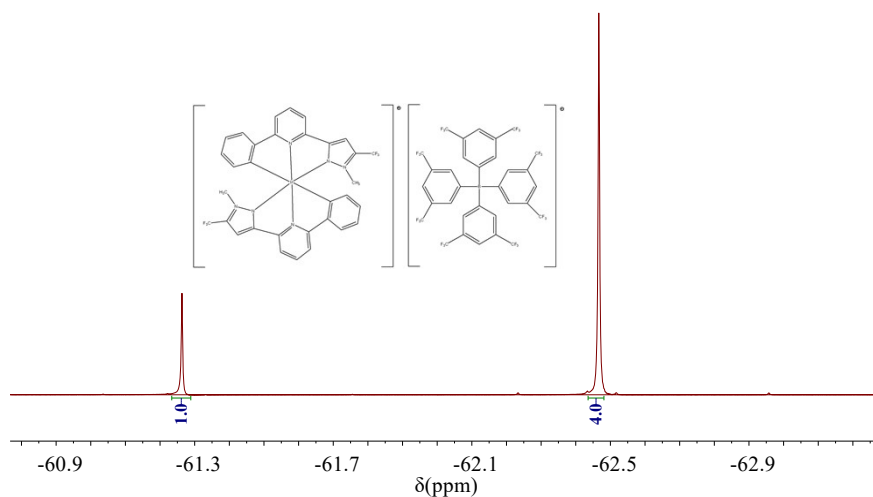
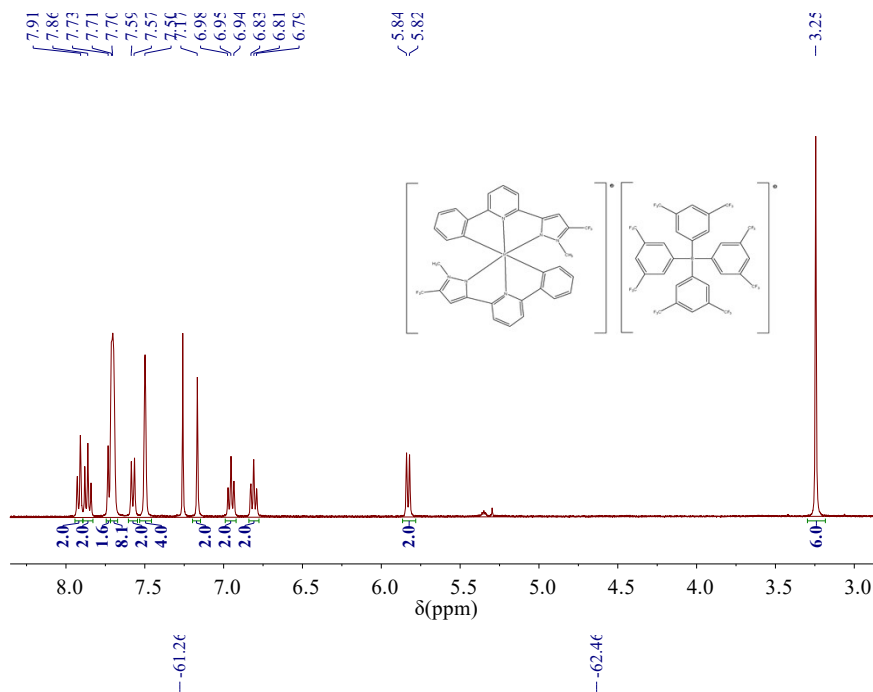
Fig. S5 (a) Electroluminescence spectra of the doped devices based on complex **2**. (b) Current density-voltage-luminance (J-V-L) characteristics of devices. (c) The current efficiency-luminance-power efficiency characteristics of devices. (d) The EQE-luminance characteristics of devices.

Table S2 Summary of device luminescence and efficiency data of complex **2**.

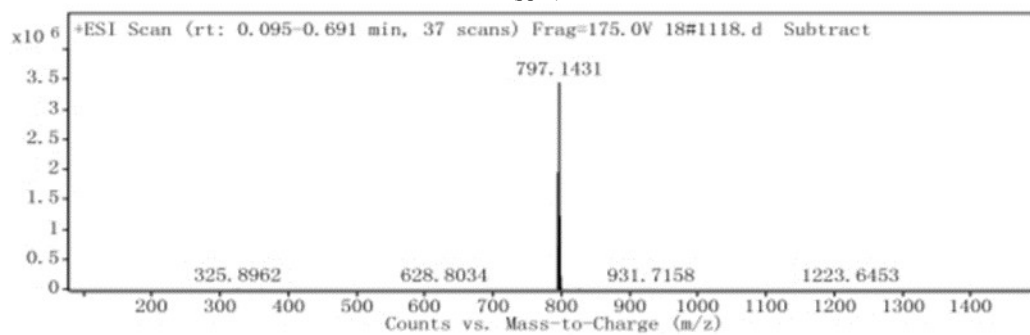
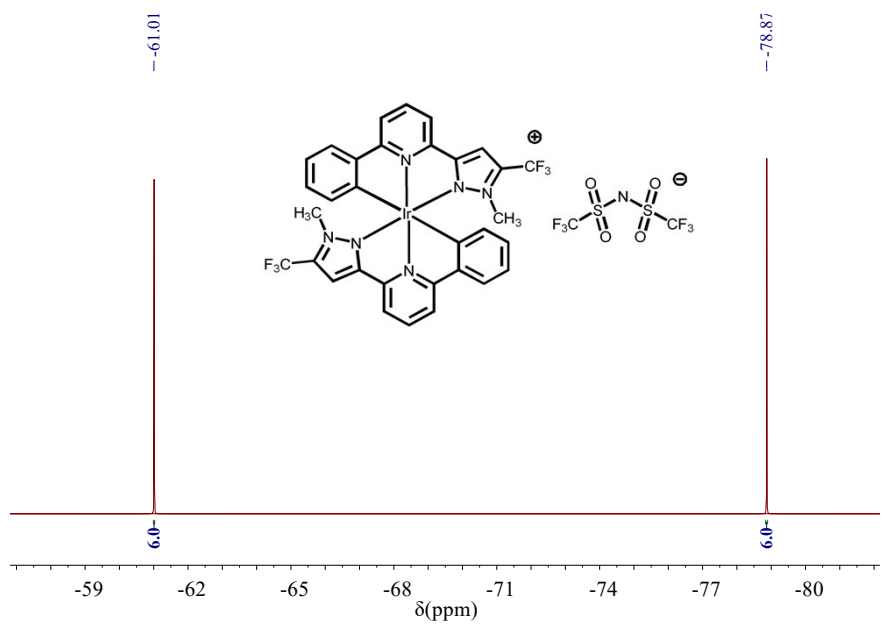
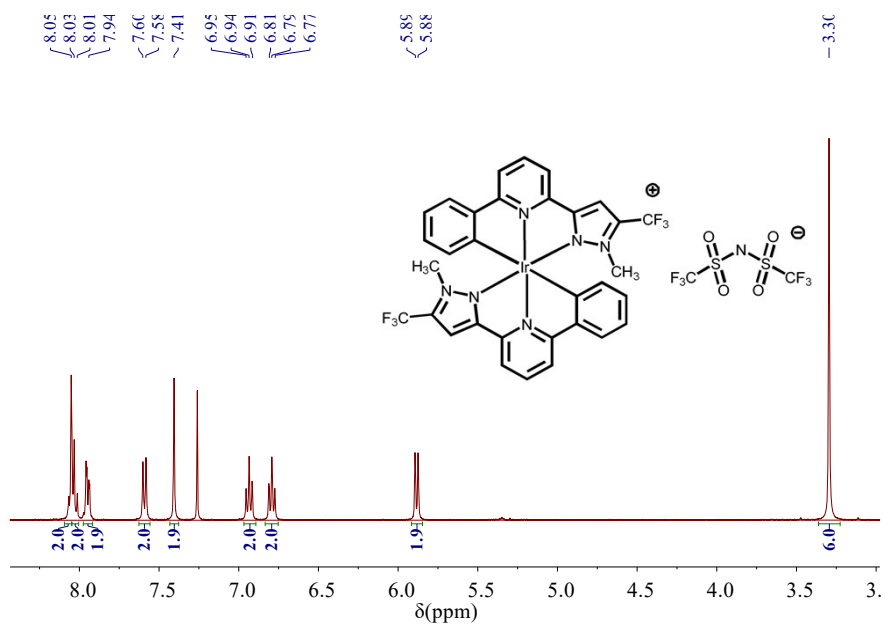
Device (content)	λ_{EL} (nm)	V_{on} (V)	L_{max} (cd/m ²)	CE_{max} (cd/A)	PE_{max} (lm/W)	EQE_{max} (%)	$CIE_{x,y}$ coordinates
S1 (0.5%)	514	5.6	30137	47.0	15.5	17.2	(0.38, 0.54)
S2 (1%)	488	6.5	1092	36.8	6.6	14.1	(0.27, 0.50)
S3 (3%)	490	7.6	3251	7.4	1.6	2.5	(0.31, 0.51)
S4 (5%)	490	9.6	1353	7.4	1.4	2.8	(0.35, 0.51)
S5 (10%)	536	9.5	764	2.0	0.7	0.8	(0.38, 0.52)
S6 (15%)	578	9.1	324	5.4	1.3	2.2	(0.42, 0.50)

5. The $^1\text{H}/^{19}\text{F}$ NMR and high-resolution mass spectrometers (HRMS) spectra of all new compounds

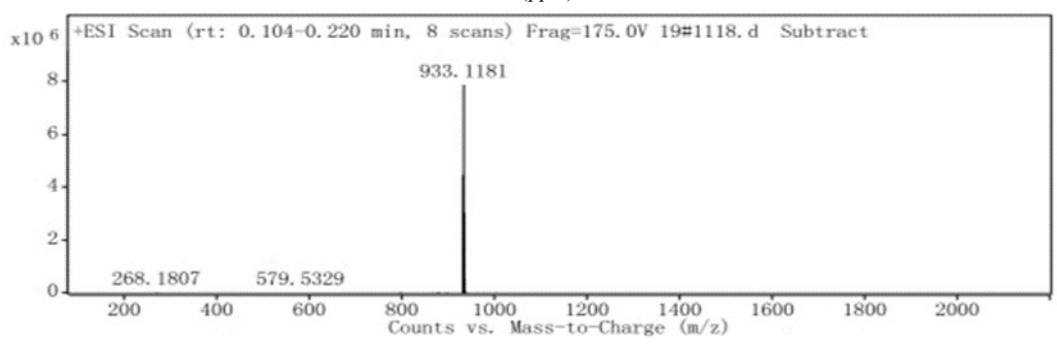
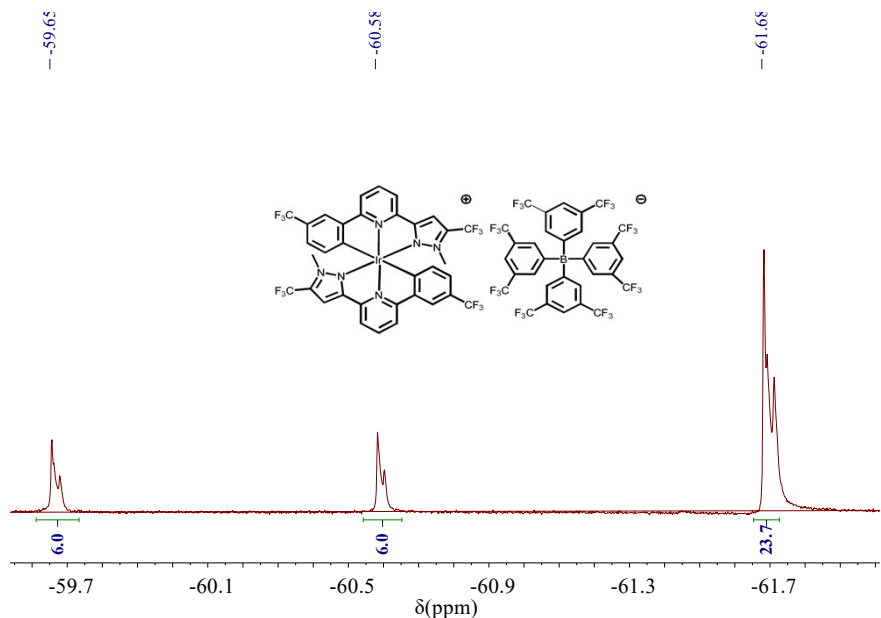
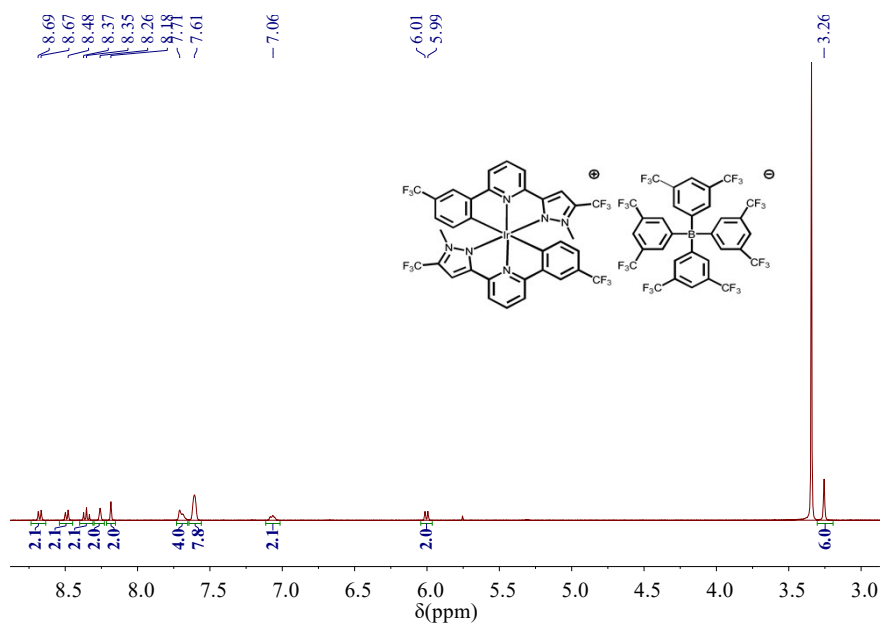
1a:



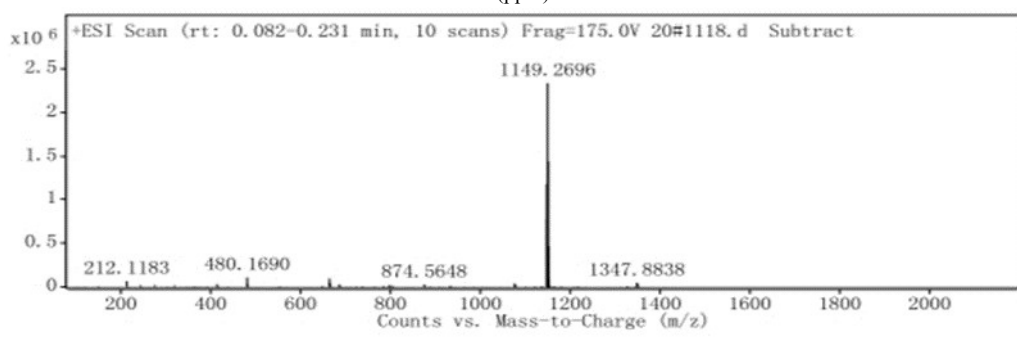
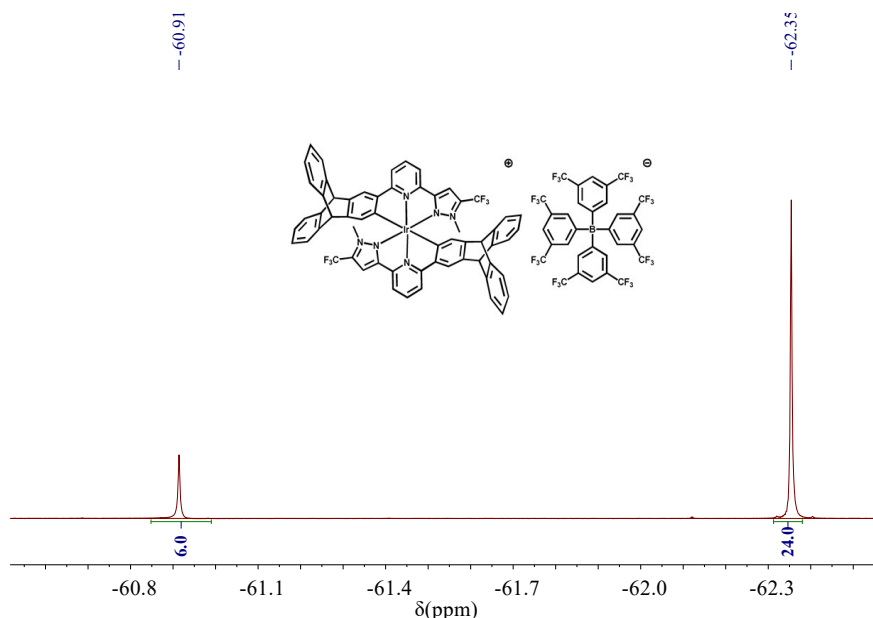
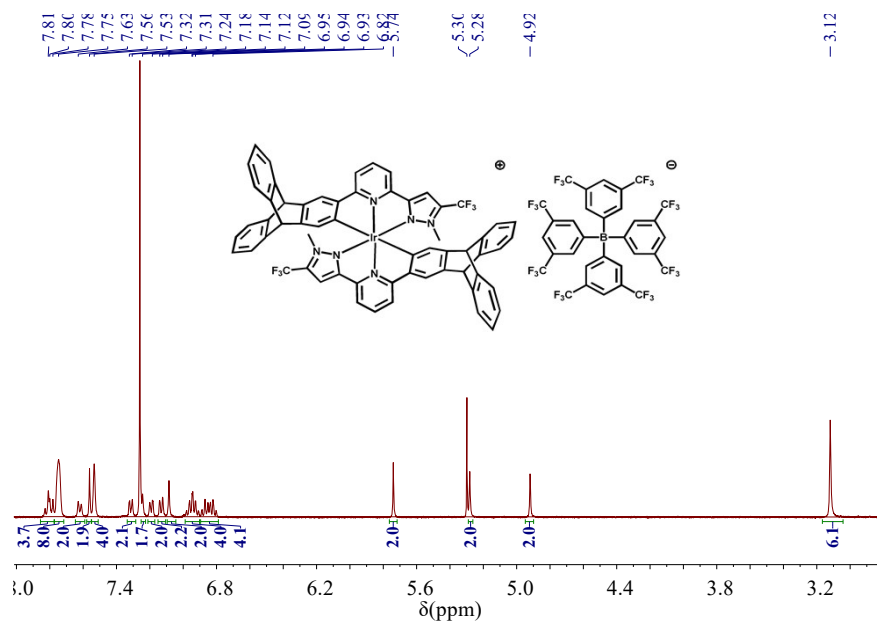
1b:



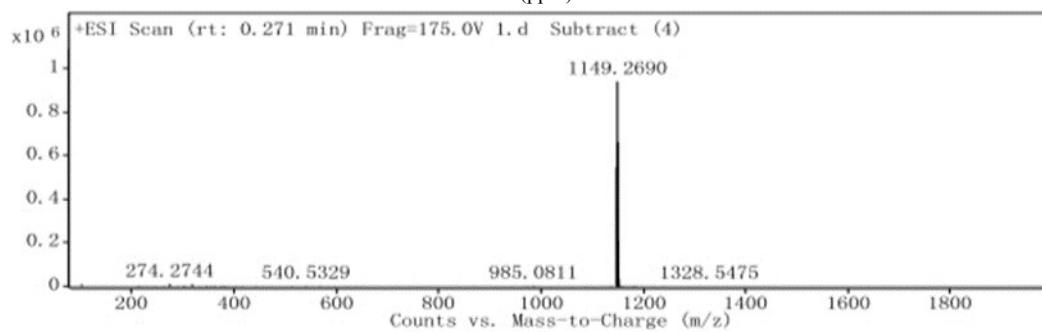
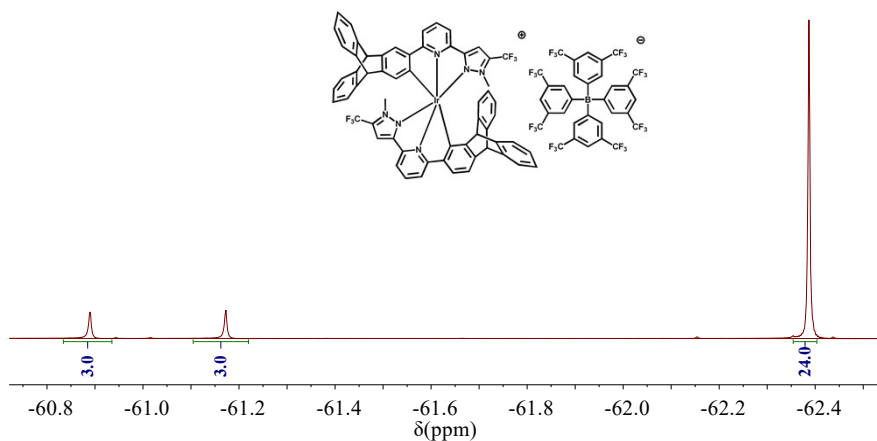
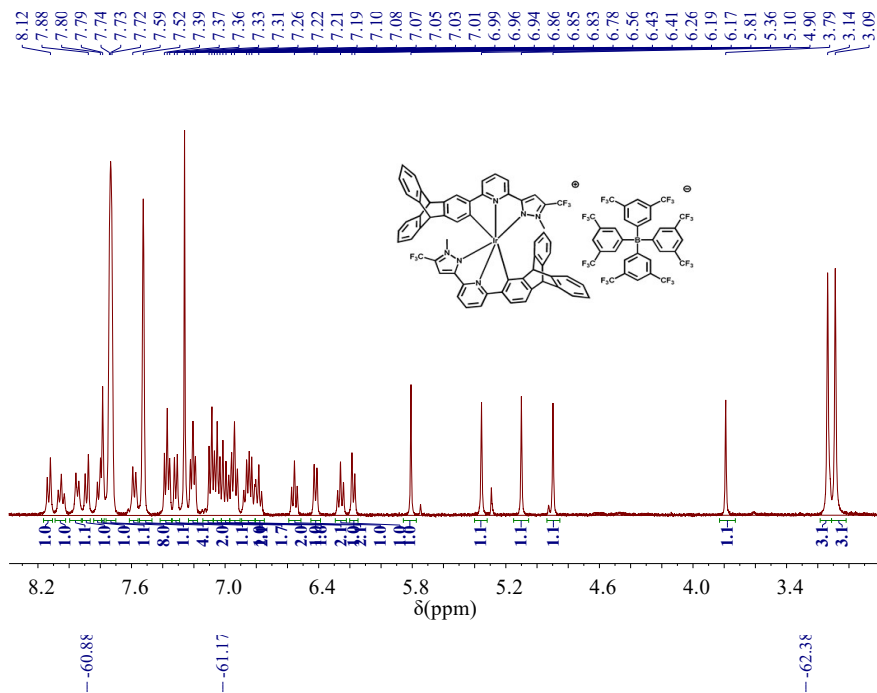
2:



3:



4:



6. References

- [1] Becke AD. Density-functional thermochemistry. III. The role of exact exchange, *J Chem Phys*, 1993; 98: 5648–5652; b) Lee C, Yang W and Parr RG. Development of the Colic-Salvetti correlation-energy formula into a functional of the electron density. *Phys Rev B*, 1988; 37:

785–789.

[2] Hay PJ and Wadt WRJ. Ab initio effective core potentials for molecular calculations. Potentials for the transition metal atoms Sc to Hg. Chem Phys, 1985; 82: 270–283; b) Wadt WR and Hay PJJ. Ab initio effective core potentials for molecular calculations. Potentials for main group elements Na to Bi. Chem Phys, 1985; 82: 284–298; c) Hay PJ and Wadt WR. Ab initio effective core potentials for molecular calculations. Potentials for K to Au including the outermost core orbitals. J Chem Phys, 1985; 82: 299–310.

[3] Hariharan PC and Pople JA. Accuracy of AH n equilibrium geometries by single determinant molecular orbital theory. Mol Phys, 1974; 27: 209–214.

[4] Lu T and Chen FW. Multiwfn: a multifunctional wavefunction analyzer. J Comput Chem, 2012; 33: 580–592.

[5] Humphrey W, Dalke A and Schulten K. VMD - visual molecular dynamics. J Molec Graphics, 1996; 14: 33–38.

[6] Frisch MJ, Trucks GW, Schlegel HB, Scuseria GE, Robb MA, Cheeseman JR, et al. Gaussian 16, Rev. B.01, Gaussian, Inc., Wallingford CT, 2016.